REPORT

International Parallel Tests on Bender Elements at the University of Porto, Portugal

Cristiana Ferreira

PhD student, Research Assistant [cristiana@fe.up.pt]

António Viana da Fonseca

Associate Professor, Director of LabGEO of FEUP [viana@fe.up.pt]

FEUP, January 2005

1   Introduction

The Geotechnical Laboratory (LabGEO) of the Faculty of Engineering of the University of Porto (FEUP) is one of the participants of the INTERNATIONAL PARALLEL TEST ON THE MEASUREMENT OF Gmax USING BENDER ELEMENTS, organized and supported by the Technical Committee TC-29 of ISSMGE. This initiative promotes the participation of institutions and laboratories worldwide currently using this state-of-the-art technique, in a series of bender element tests using the well-known Toyoura sand (from Japan), according to pre-established specifications. The aim of the International parallel tests using bender elements is to disseminate the experience of different practices (in terms of data acquisition, analysis and interpretation of results) used worldwide and to develop the recommendation for procedures referred to bender elements test.

The present report describes and details the results obtained for a short series of tests carried out at the Geotechnical Laboratory of FEUP, under the specified testing procedures.

2   Background of bender element testing at LabGEO of FEUP

The LabGEO of FEUP has been using bender elements, since 2000, when a recently acquired triaxial system equipped with bender elements and compression transducers, from ISMES-Enel.Hydro, was set up and put into operation. Subsequently, another conventional triaxial cell was locally modified and new bender and extender elements were implemented. These piezoelectric transducers originated from the University of Bristol, where significant efforts on the development of these devices were being made, under the supervision of Dr. David Nash and colleagues (Viana da Fonseca & Ferreira, 2002).

These equipments have been continuously in use, mainly for research purposes. The first and most important application of this testing technique has been the comparative assessment of sampling quality on young residual soils from granite. This technique proved to show substantial differences on shear wave velocity V_s, hence shear modulus G_{max}, of samples retrieved by different samplers, with distinct induced disturbances (Ferreira et al., 2004).

The other research topic involving bender elements has been the issue of interpretation of the measurements. It is widely accepted that there is some uncertainty in the interpretation of the bender element traces and that however simple the transmitter wave is, a far more complex wave will be received (Moncaster, 1997).

For this purpose, an extensive set of tests mainly on natural residual soils has been performed, using different interpretation methods, in order to further understand the differences in the results, towards determining which method most closely estimates the true travel time.

In this framework of research, it is therefore with enthusiasm and great expectations that the LabGEO of FEUP has embraced this initiative.

3   Outline of the test apparatus

The triaxial test apparatus was used for carrying out these tests. Cylindrical samples of Toyoura sand were tested, with 70mm diameter and 140mm height.

The triaxial testing device, equipped with bender elements and compression transducers, was originally developed at the Italian Research Centre *ISMES, Spa* and later commercialized by the company *Enel.Hydro*. Besides the triaxial chamber itself, this system consists of a very simple pressure control panel, a function generator, an input-output amplifier with data acquisition and an oscilloscope. The confining pressure is applied by means of an air-water

interface, inside the chamber, where the compressed air is regulated in the control panel. Figure 1a shows this apparatus in use at the LabGEO of FEUP.

a)   b)
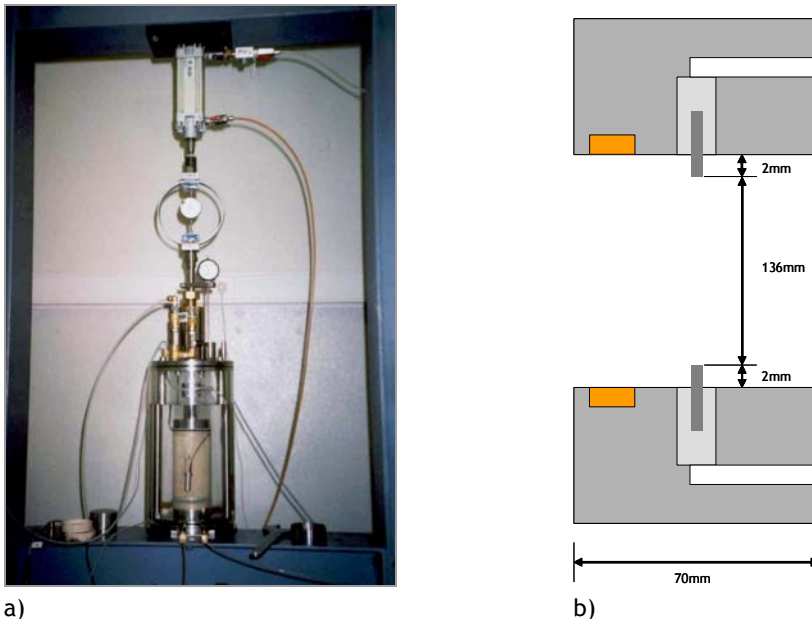
Figure 1 – Triaxial apparatus at LabGEO of FEUP:
a) triaxial chamber; b) scheme of the tip-to-tip distance and protrusion of the bender elements

4   Details of the bender elements

In terms of the piezoelectric transducers, only the bender elements will be hereby detailed. The bender elements have been provided already mounted in the platens of the triaxial cell. Each bender element consists of two plates glued together and polarised so that, when stressed by an electrical signal, one elongates and the other contracts. According to the manufacturer, the dimensions of the transducers are about 20mm x 10mm with a thickness of 3mm. It is possible to directly measure the protrusion of the bender elements, which is approximately 2mm on each platen. Hence, the tip-to-tip distance is calculated by subtracting 4mm to the sample height, as shown in Figure 1b.

As to the electrical connections, the manufacturer informs that the transducers can be used as transmitters or as receivers since they have been built in the same way.

The electronic equipments used for running the bender element measurements consist of:

- □ A programmable function generator *(TTi, Thurlby Thandar Instruments-TG1010)* with several wave shapes (sinusoidal, square, ramp or other) and configurations (continuous, repeating pulses, sweep, etc.);
- □ An integrated unit with input and output amplifiers (specifically developed by *ISMES-Enel.Hydro*), which automatically amplifies 40x the input voltage and

enables the selection of four levels of output amplification (1x, 2x, 5x and 10x); and,

▫ An oscilloscope (*Tektronix* TDS 220), directly connected to the amplifier unit, which records the signals and enables the immediate identification of the travel time; this device is also connected to a PC and, by means of specific software, it is possible to transfer and save the obtained results under various formats, for further analysis and interpretation;

▫ Alternatively to the oscilloscope, a data acquisition wit spectral analysis device has been used (*PICOScope* ADC 216), also connected to a PC, where specifically designed software was used for acquisition and control.

In Figure 2, a photograph of the transducers and a simplified scheme of the layout of the elements of the bottom platen are presented.
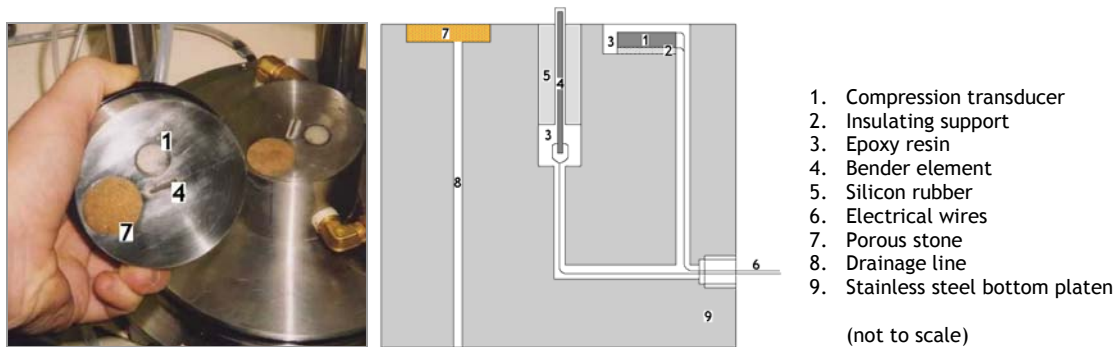

1. Compression transducer
2. Insulating support
3. Epoxy resin
4. Bender element
5. Silicon rubber
6. Electrical wires
7. Porous stone
8. Drainage line
9. Stainless steel bottom platen

(not to scale)

Figure 2 – Compression transducers and bender elements in the triaxial cell

5   Test description and procedure

For this International Parallel Test series on bender element measurements, three extensive tests have been considered valid, named RR1, RR2 and RR3. The test procedure specifications provided were closely followed. Details of each test can be found in the respective test form attached.

Toyoura sand samples were air pluviated, resulting on void ratios of about 0.70. All these samples were dry throughout testing. Four isotropic stress stages (50, 100, 200 and 400 kPa) were applied, according to the instructions provided. The nomenclature used to designate each test stage was "StageNumber-TestName"; for example, the third stage (200kPa) of the second test is "03-RR2".

6 Interpretation of bender element measurements

Time and frequency domain measurements were taken, for the application of the different interpretation methods, namely:

- First direct arrival, at various frequencies
- Discrete method of phase frequencies [π points]
- Continuous sweep input frequency [ABETS]

In what follows, each of these techniques will be briefly described.

6.1 Time domain

First direct arrival method, at various frequencies [time domain]

The first direct arrival method is the most simple, common and usual procedure for interpreting bender element measurements. It consists on the identification of the first instant of arrival of the wave in the output signal, similarly to the techniques used in geophysical tests (namely Cross-Hole and Down-Hole). While it is sometimes easy to determine first arrival, it is often the cause of much uncertainty. For instance, Arroyo (2001) has estimated uncertainties of up to 100% in estimation of the small strain shear stiffness (G_{max}). Many authors (Sanchez-Salinero et al., 1986; Viggiani & Atkinson, 1995; Jovičić et al., 1996; Arulnathan et al., 1998) have reported several sources and factors of error and inherent near field effects, which mask and compromise the identification of the arrival point.

Figure 3 exemplifies a typical bender element trace, where the arrival instant can be determined within a margin of error of about 20%.
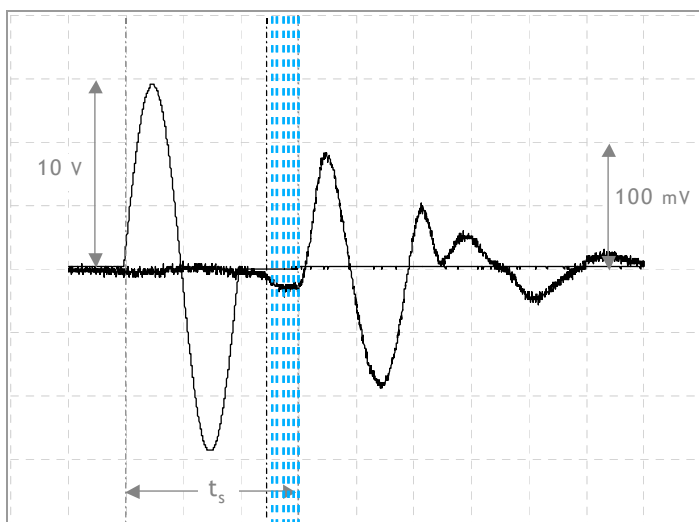

Figure 3 – Determination of the travel time with the first direct arrival method

Several solutions have been proposed in order to minimize the subjectivity of this method, mainly by reducing the initial distortion of the signal. This can be achieved by changing the frequency and shape of the input wave, whilst ensuring the accomplishment of a number of technical requirements and boundary conditions. According to Jovicic (2004), these technical requirements comprise:

- good electronics equipment, namely a function generator and an oscilloscope with screen;
- well shielded and grounded cables;
- properly connected and encased bender elements;
- leak free connections;
- noise free environment;

Special attention should be put on design details, leaks and wear-and-tear issues.

On the other hand, the boundary conditions refer to the spatial conditions (such as the alignment of the bender elements, the reflections of the wave on the edges of the sample, the near field effect or the relative distance between the transmitter and the receiver), the contact between the bender element and the soil (which might induce poor coupling) and the overshooting (at high frequencies, the bender element changes its mode shape and the response becomes very complex).

In the present tests, the first arrival method was used and several input frequencies at relevant levels were applied, as well as simultaneous P- and S- wave recordings, in order to take into consideration the near field effect.
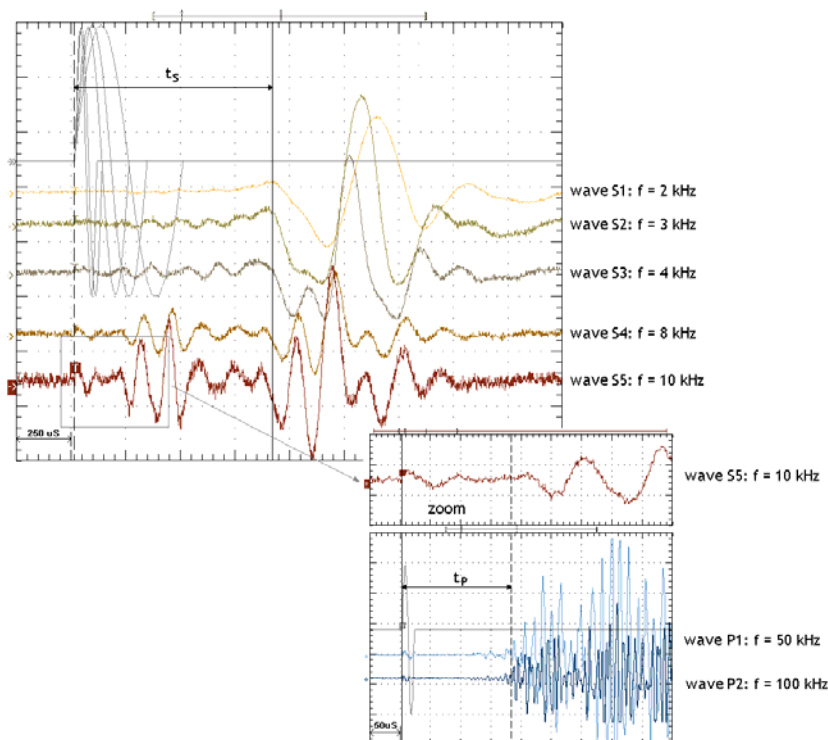

Figure 4 – First direct arrival method at various input frequencies, considering near field effect

This procedure has evidenced the presence of near field effect, enabling the identification of the compressional component of the shear wave.

It should be noted that, for all the tests carried out at FEUP, the polarity of the received wave is negative, i.e., inverted in relation to the input wave. For this reason, the first arrival point corresponds to the beginning of the first significant trough.

6.2 Frequency domain

The use of continuous signals which require the shear wave velocity to be decoded from measurements of relative phase of transmitted and received signals is gaining in popularity (e.g. Blewett et al., 1999). While the technique is used very widely across a wide range of fields, Viggiani and Atkinson (1995) were the first to apply phase-delay method to bender element testing. According to Greening et al. (2003), these methods have a number of advantages over traditional pulse-based measurements. Chief amongst these is that it is convenient to create an algorithm to determine travel time by establishing the gradient of a graph of phase difference against frequency. Phase delay methods can be performed reliably using "traditional" equipment i.e. a signal generator and oscilloscope (Kaarsberg, 1975). A continuous harmonic sinusoid is used as the input signal. The frequency of the signal is changed and the frequencies at which the transmitted signal and received signal are exactly in and out of phase with one another (so called π-points) are noted. Greening and Nash (2003) showed that same information could be established less onerously using broadband (sweep) input signal and a spectrum analyser.

Whereas the continuous sweep input method enables the acquisition of a continuous phase angle versus frequency relationship, for the discrete method only specific points can be observed, the π-points; hence, this is a simplified version of the more complete continuous sweep input frequency method.

In the present work, for the frequency domain, two different methods were considered: the discrete method of phase frequencies and the continuous sweep input frequency.

Discrete method of phase frequencies [π points]

The discrete method of phase frequencies method consists on the identification of the π-points, i.e., the frequencies to which the input and output signals are either in or out of phase. The phase angle corresponds to a measure of this relation between the input and the output signals, taking a value multiple of π, when an in or out of phase relation occurs.

In the absence of spectral analysis equipment, the identification of the phase frequencies is performed manually, by defining discrete points to which the phase angle is known to be multiple of π. The sequence procedure for the application of this simplified approach to the frequency domain can be divided in the following stages:

- Input of a continuous sine wave, at a very low frequency, from the function generator;
- Selection of a XY display in the oscilloscope;
- Slow and gradual increase of the input signal frequency, until a relation between the two input and output waves is clearly visible (similar to any in Figure 5);
- Registration of the frequencies values of the π-points, defined by the observation in the oscilloscope of the Lissajous figures (Figure 5), when the relation of the two waves becomes linear; this process is repeated for as long as it can be clearly observed (generally no further than 20kHz):

$$\text{In- and out-of-phase frequencies: } \phi(f) = k\pi$$

- Plot of these frequency values versus the respective number of wavelengths N, which increase sequentially of 0.5 in each phase frequency; since the slope is only dependent on the relative difference between the ordinates and, as long as the sequential increase of 0.5 is maintained, the absolute value of the first N can be arbitrary;

$$\text{Number of wavelengths: } N = \frac{L}{\lambda} = \frac{L \cdot f}{V} = \frac{\phi(f)}{2\pi} = \frac{k}{2}$$

- Determination of the average slope of the obtained plot, defined by linear regression of all, or a selection of, the points of the plot; the slope value coincides with the travel time.

$$\text{Wave velocity: } V = \lambda \cdot f = 2\pi \cdot f \frac{L}{\phi(f)}$$

$$\text{Travel time: } t = \frac{L}{V} = \frac{N}{f} \quad (\equiv \text{slope})$$
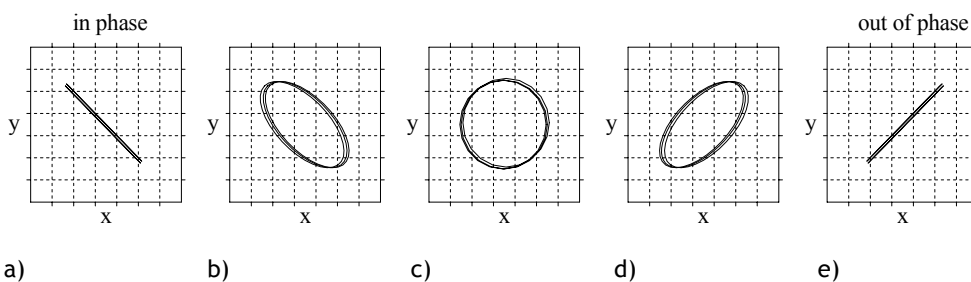

Figure 5 – Different oscilloscope XY displays of the transmitted and received signals (Rio, 2002)

A typical result of the application of this method is illustrated in Figure 6. The phase frequencies curve is practically linear, providing good confidence in the travel time derived from its slope.
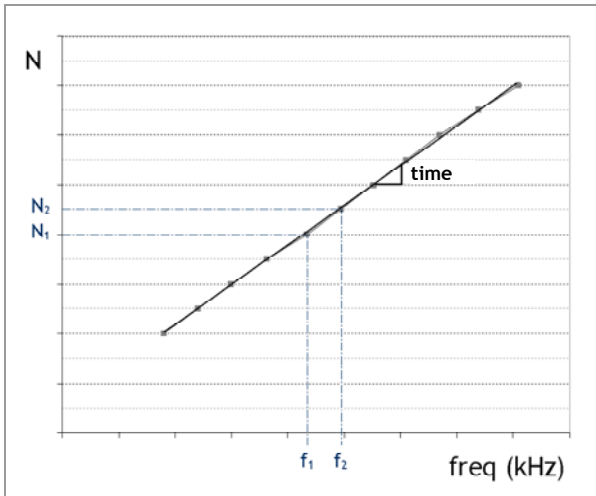

Figure 6 – Frequency versus number of wavelengths: the slope is the travel time

Continuous sweep input frequency [ABETS]

Following Greening et al. (2003) setup, a low-cost spectrum analyser system has been implemented in *Microsoft Excel*^{TM}, which uses the functionality of the PC on which specific software is loaded and controls a PICO high-speed dual channel data acquisition unit. The software has been called ABETS (Automatic Bender Element Testing System). A schematic of the system is shown in Figure 7a. The software was originally developed by Dr. Paul Greening at UCL and details on how data is processed can be found in Greening et al. (2003). Slight modifications have been introduced to the program, namely for post-processing data. A screenshot of this program, in its Portuguese version, is presented in Figure 7b.

a)   b)
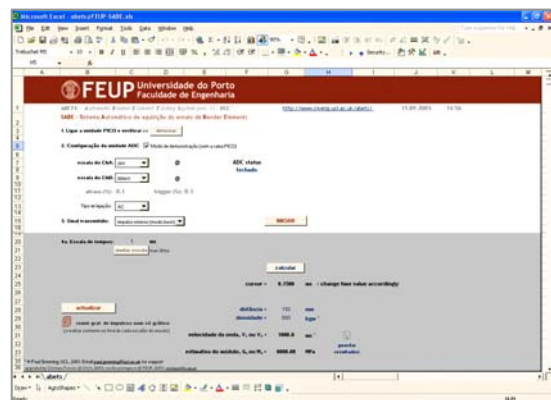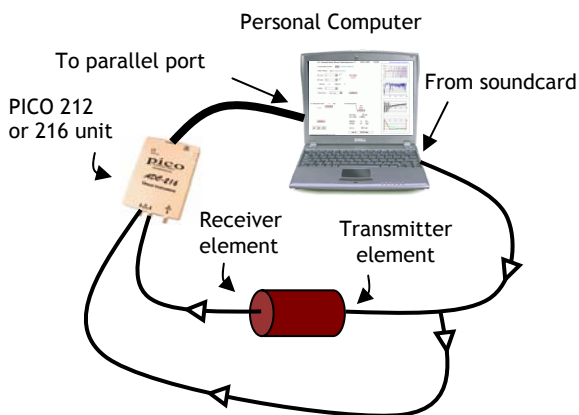
Figure 7 – a) Schematic of the PC based spectrum analyser for bender element testing (from Greening et al., 2003); b) Screenshot of the Portuguese version, at FEUP

Best results have been obtained with a sweep sine signal with a 0-20kHz bandwidth. An example of the data acquisition results spreadsheet is given in Figure 8. The first graph shows the input and output signals in the time domain, where it is impossible to determine a direct arrival time. Below is the coherence function (from 0 to 1) between the two signals against input frequency, which provides indications of the correlation of those signals. The higher the coherence, the more correlated the signals will be. The plots at the right show the relative phase against frequency; in the top one, the phase angle is "wrapped", ranging from -π to π, while on the bottom one, it is "unwrapped", starting nearly at zero and continuously increasing. This graph is similar to the one in Figure 6 (apart from the y-axis units) and similarly to that, the travel time is derived from the slope of the curve, taken from the best fit line.
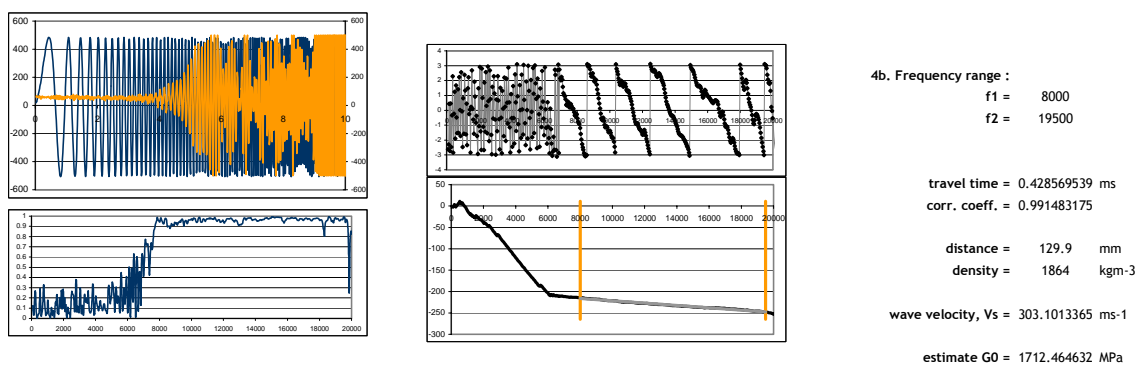

Figure 8 – Data acquisition results using ABETS

A few practical observations should be made regarding the interpretation of the acquired data. Firstly, a non-linear relationship between the relative phase and the signal frequency can be seen. In all tests carried out, it was observed that the 0-20kHz range is too wide to provide reasonable results. However, it is useful to get an overview of the full coherence function as well as the complete unwrapped phase against frequency relationship, with the purpose of deciding the most adequate ranges to select.

Therefore, a selection of a high coherence range is usually necessary in order to have a reliable unwrapping and low dispersion in the results, thus a high correlation coefficient of the best fit line. Such selection is evidenced in the vertical lines of the bottom right graph, between which the travel time has been computed.

Usual practice suggests that after the test is conducted, further analyses are carried out, mainly by selecting different ranges of frequencies in order to observe any changes in the travel time. As the previous figure shows, a few "lumps" and "bumps" are visible even in the selected range. This means that a higher correlation can be obtained if a narrower range is selected, avoiding those disturbances in the curve.

7   Overview of the results

A brief summary of the obtained results will be presented in this section. All the information is compiled in the test forms and the test stage files, attached to this document.

a) First direct arrival, at various frequencies

For the three tests, the application of the time domain has provided similar trends despite some variation on RR3, as the following graph shows for the calculated maximum shear modulus versus the isotropic effective stress.
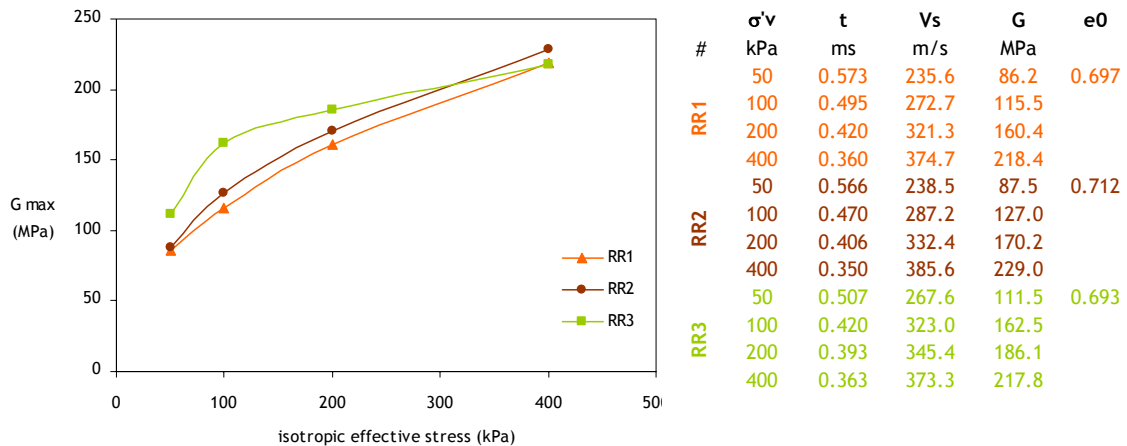
#	σ'v kPa	t ms	Vs m/s	G MPa	e0
RR1	50	0.573	235.6	86.2	0.697
	100	0.495	272.7	115.5	
	200	0.420	321.3	160.4	
	400	0.360	374.7	218.4	
RR2	50	0.566	238.5	87.5	0.712
	100	0.470	287.2	127.0	
	200	0.406	332.4	170.2	
	400	0.350	385.6	229.0	
RR3	50	0.507	267.6	111.5	0.693
	100	0.420	323.0	162.5	
	200	0.393	345.4	186.1	
	400	0.363	373.3	217.8	

Figure 9 – Time domain results for the 3 tests

In general, the identification of the first arrival instant required careful observation and for all test stages, groups of three or four different input frequencies was used and compared to ease the interpretation process, as illustrated in Figure 10.
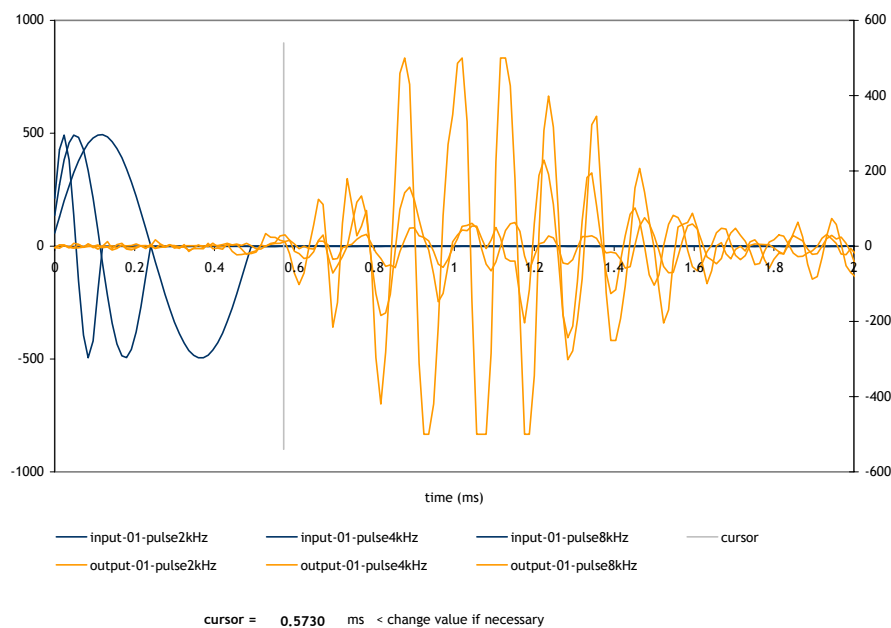
Figure 10 – First arrival results for the 1st stage of RR1

In this case, the travel time from the pulse measurements considered individually, has led to:

2 kHz   0.591ms

4 kHz   0.573ms

8 kHz   0.570ms   >> selected value for all pulses: 0.573ms

This example shows slight variations in the travel time according to the input frequency, of about 4%, which is negligible and fully acceptable.

b) Discrete method of phase frequencies [π points]

As previously stated, this method consists on a more rudimentary and onerous version of the continuous sweep input frequency. For that reason, it was only applied for RR3, as a means to compare and confirm the coincidence of results.

In the following graph, the results for the 1st and 3rd stage of RR3 using the π-point method and ABETS have been put together. This example clearly demonstrates that these methods provide identical results, in terms of the overall slope of the curve, whilst evidencing a much wider and informative range for the case of the sweep results.
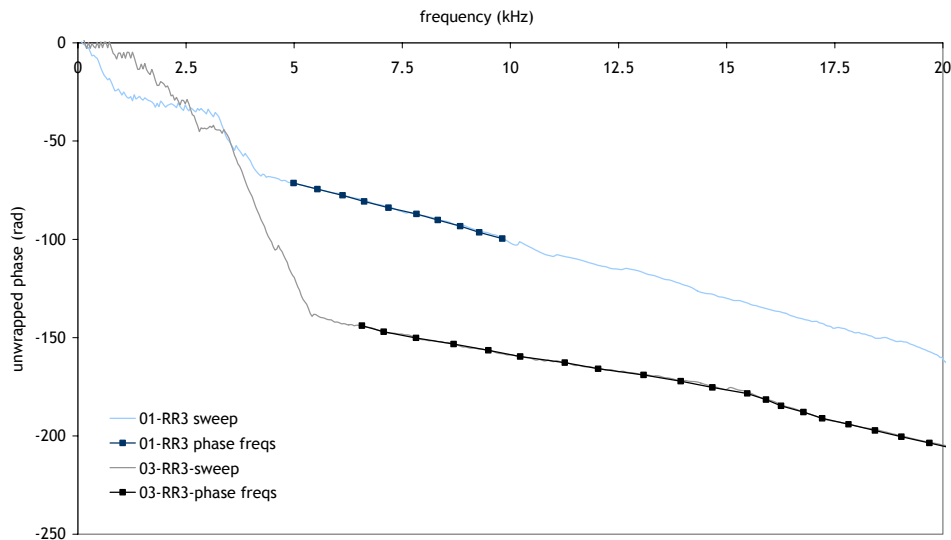

Figure 11 – Results of the π-point and sweep methods for 2 different stages of RR3

c) Continuous sweep input frequency [ABETS]

The results of the application of this interpretation method, on these tests using Toyoura sand, have been substantially different from what was originally expected, as will be illustrated in the following example.

From the sweep input method, and for the same test stage [01-RR1] previously detailed in the first arrival, the results were:

0-20 kHz	1.250ms	> discarded, due to the coherence variation
5-10 kHz	1.040ms	> 1st choice
6-19 kHz	0.566ms	> low correlation coefficient: visible "lump" in the plot
9-18 kHz	0.351ms	> low correlation coefficient: visible "lump" in the plot

In the test forms, only relevant selections of the frequency ranges are reported, i.e., the full range 0-20 kHz has not been considered. Nevertheless, the differences are quite substantial. In fact, the closest value to the first arrival result corresponds to a range with low correlation coefficient, where clear shifts in the slope can be seen, hence on the travel time.

In this first stage of the first test, the changes in the travel time according to the selected range of frequencies were extremely high, of more than a factor of 3, exceeding the worst-case scenario. This also indicated unexpected subjectivity associated with the choice of frequencies which had not been observed in any previous tests, on different geomaterials. At least, that was the case for the labGEO of FEUP.

With the purpose of further understanding this dispersion and variation of travel times using continuous readings, another approach has been investigated. This consists on a different method of representing the travel time from the sweep results. A simple Visual Basic program was implemented, to manipulate the sweep data considering "unbiased" and objective pre-established ranges of frequencies, in order to calculate the minimum square method for the respective best fit line. The initial range fittings were 0.2, 0.5, 1, 2, 4 and 6 kHz. The generated graph of travel time versus frequency, called "time chart", is presented in Figure 12, where the corresponding first arrival results are included, for the respective frequency range.

Firstly, the graph evidences that the lower ranges, of 0.2 and 0.5 kHz, are very sensitive and strongly affected by noise. From this observation, the 0.2 kHz range has not been removed and the 0.5 kHz range has been left as reference to the original data trends.

The present example confirms the very high variability previously identified for the selected ranges. It reveals the complexity of the range selection and its immediate effect on the resulting travel time. It should be mentioned, however, that all other test stages exhibit much less variability, so this is really the most difficult and extreme observed situation.

In order to understand what might be affecting the results so much, it is interesting to look at the coherence function of frequency graph. There is significant correspondence between the variability of the two plots. The coherence evidences various zones of low values and, most of all, an erratic shape. This might partly justify the inconsistencies of the time chart.
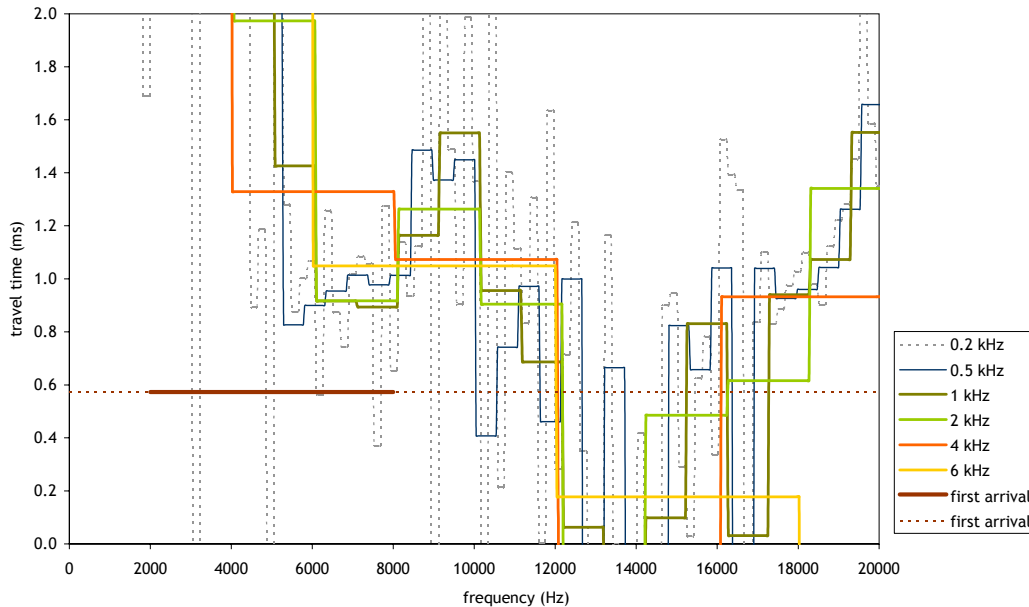

Figure 12 – Time charts for selected range fittings (0.2, 0.5, 1, 2, 4 and 6 kHz) for 01-RR1
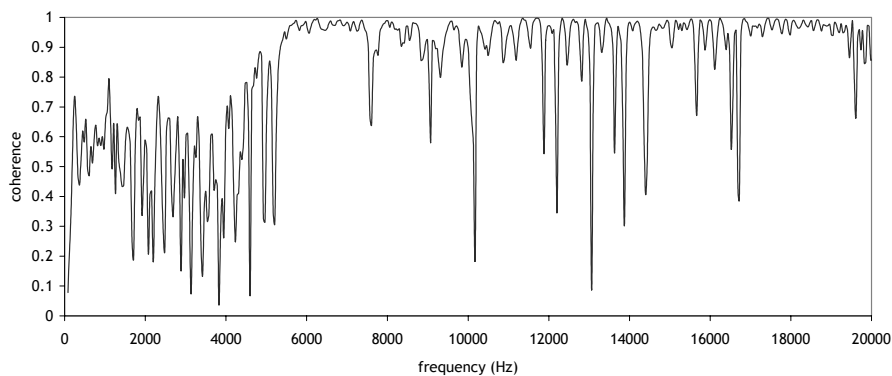

Figure 13 – Coherence function for test stage 01-RR1

In each test stage file attached, the respective time chart is provided. It can be noted that the fluctuations of travel time with frequency for the various ranges decrease substantially with the stress increase, as well as the relative distance to the travel time measured by the first arrival method. This fact is likely to be associated with a higher coupling between the soil and the bender elements.

As proof of a much more balanced time chart, the following figure shows the one obtained for test stage 04-RR1.
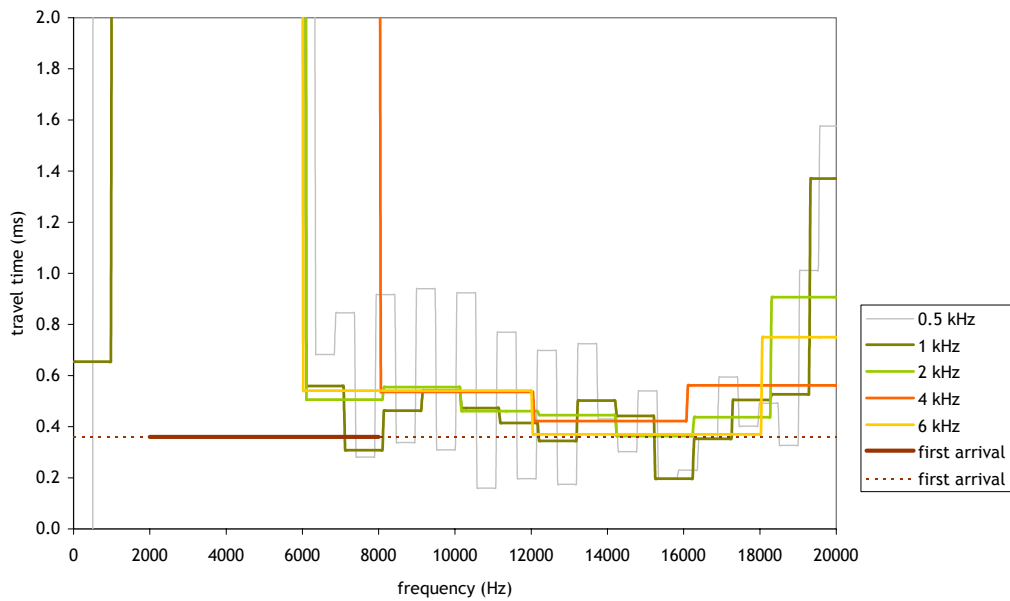
Figure 14 – Time charts for test stage 04-RR1

Besides enabling an overview of the travel time in a continuous manner, the time chart also represents a new, useful and practical way of selecting the most adequate travel time, with less iterations and error. Therefore, it is clearly an improvement of the sweep method. Having been conceived in an attempt to understand the first and most complex test results, it is at this point considered a fortunate fruit of such incident.

8   Discussion of the interpretation methods

The first important conclusion to be derived from this exercise is that the results from the frequency domain vary significantly for slight changes in the frequency range, meaning that the use of these methods may require an educated judgement and a critical assessment of the obtained values.

As a final comparison, the travel time results for the time domain and the frequency domain have been gathered in a graph against the applied isotropic effective stress, shown in Figure 15.

The convergence of the results in the higher stresses is evident. Despite following similar trends, the comparison between the different interpretation methods results in repetitive tests is not conclusive. In fact, the differences in the results for the first stress stages are quite variable among the three tests. While the RR1 test, the difference between the two domains is almost double, for RR2 it is less than 20%. Bearing in mind that these tests were carried out in identical samples, there is certainly room for further investigations.
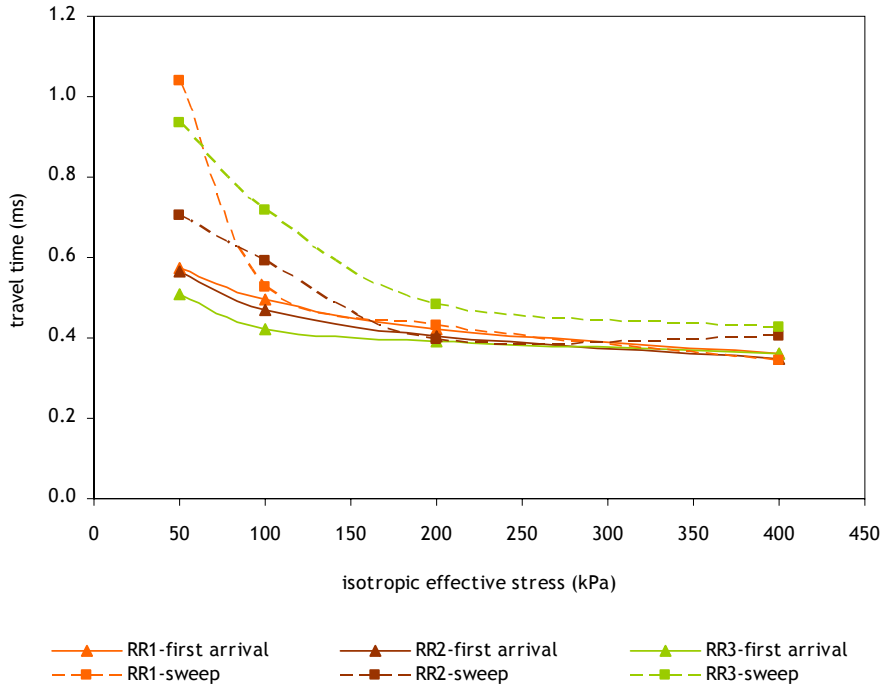
Figure 15 – Travel time results for all tests, in the time and frequency domains

Such discrepancies in the results clearly inform that there is still much to understand regarding how the input wave travels within the sample, whether and how much of it is reflected in its boundaries, and how it is picked up by the receiver on the other end.

In our opinion, these series of tests have shown much uncertainty and many of the fragilities in the currently available interpretation methods. Nevertheless, these have also led to a continuing and renovated interest in a deeper research on this innovative and promising laboratory test.

It should be pointed out that, alike all other testing equipments and technologies, there is a scope of materials and conditions to which the response of the system is more reliable and adequate. Outside that scope of applicability, there is a high probability of inconsistent results. We do not know whether this is the case for the bender element testing method. In any case, other geomaterials have been tested at labGEO of FEUP as well as in other laboratories, which show less dispersive and complex results.

From this exercise derives the need to understand in greater depth how the input wave is actually traveling within the sample and the urgency to know the right track, whether it is the time or the frequency domain, or any other.

9 References

Arroyo, M. (2001). *Pulse tests in soil samples.* PhD Thesis University of Bristol, UK.

Arulnathan, R.; Boulanger, R.W.; Riemer, M.F. (1998). *Analysis of bender element tests.* Geotechnical Testing Journal, Vol. 21, No. 2, pp. 120-131.

Blewett J, Blewett I. J. & Woodward P.K (1999). *Measurement of shear wave velocity using phase sensitive detection techniques.* Canadian Geotechnical Journal, No. 36, pp. 934-939.

Ferreira, C.; Mendonça, A.A. & Viana da Fonseca, A. (2004). *Assessment of sampling quality in experimental sites on residual soil from granite in Porto (in Portuguese).* Proceedings of the 9th Portuguese Geotechnical Congress, Aveiro, Portugal, SPG, Lisboa, Vol. 1, pp. 27-38.

Greening, P. D.; Nash, D. F. T.; Benahmed, N.; Ferreira, C. & Viana da Fonseca, A. (2003). *Comparison of shear wave velocity measurements in different materials using time and frequency domain techniques.* Proceedings of the 3rd International Symposium on Deformation Characteristics of Geomaterials, IS-Lyon '03, France. September 2003. Di Benedetto et al. (Eds). Swets & Zeitlinger, Lisse. Vol. 1, pp. 381-386.

Greening, P.D & Nash, D.F.T. (2003). *Frequency domain determination of G0 using bender elements.* ASTM Journal of Geotechnical Testing.

Jovičić, V. (2004). *Rigorous bender element testing.* Workshop on Bender Element Testing of Soils, UCL, London.

Jovicic,V.; Coop, M.R.; Simic, M. (1996). *Objective criteria for determining Gmax from bender element tests.* Géotechnique, Vol. 46, No. 2, pp. 357-362.

Kaarsberg, E.A. (1975). *Elastic-Wave Velocity Measurements in Rocks and Other Materials by Phase-Delay Methods.* Geophysics No.40, pp. 955-901.

Moncaster, A.M. (1997). *The shear modulus of sand at very small strains.* MSc thesis. Department of Civil Engineering, University of Bristol, UK.

Rio, J. (2002). *Advances in laboratory geophysics using bender elements.* Internal Report, University College London.

Sánchez-Salinero I., Roesset J.M. & Stokoe II K.H. (1986). *Analytical studies of wave propagation and attenuation* Geotechnical report

Viana da Fonseca, A. & Ferreira, C. (2002) *Bender elements: excelent laboratory techniques for the evaluation of referencial geotechnical parameters (in Portuguese).* Proceedings of the 8th Portuguese Geotechnical Congress, LNEC, Lisboa

Viggiani, G. & Atkinson, J.H. (1995). *Interpretation of bender element tests.* Géotechnique, Vol. 45, No.1, pp.149-154.